Preprint Title	Alcohol-Perturbed Self-Assembly of Tobacco Mosaic Virus Coat Protein
Authors	Ismael Abu-Baker and Amy S. Blum
Publication Date	05 Jan. 2022
Article Type	Full Research Paper
Supporting Information File 1	Supporting Information.docx; 10.3 MB
ORCID® iDs	Ismael Abu-Baker - https://orcid.org/0000-0001-8286-8484

Alcohol-Perturbed Self-Assembly of Tobacco Mosaic Virus Coat Protein

*Ismael Abu-Baker, Amy Szuchmacher Blum**

Department of Chemistry, McGill University, Montréal, Québec, Canada

Abstract

Self-assembly of Tobacco mosaic virus coat protein is significantly altered in alcohol-water mixtures. Alcohol cosolvents stabilize the disk aggregate and prevent formation of helical rods at low pH. High alcohol content favours stacked disk assemblies and large rafts, while low alcohol concentration favours individual disks and short stacks. These effects appear to be caused by the hydrophobicity of the alcohol additive, with isopropyl alcohol having the strongest effect, and methanol the weakest. We hypothesize that alcohols interact with the hydrophobic faces of TMV-cp disks, thereby disrupting the protein-protein interactions between disks that are necessary to form helical rods.

Introduction

Bottom-up fabrication of nanomaterials with precise control over the spatial arrangement of components is of great interest in nanotechnology.[1] A promising approach to this issue is the use of templates based on self-assembling biological materials, such as nucleic acids and proteins.[2,

3] Such biological scaffolds can be programmed through predictable chemical interactions to form complex, well-defined nanostructures. Viruses and virus-like particles (VLPs) possess many advantageous properties for biotemplating applications.[4, 5] Native viruses are highly monodisperse due to the encapsidated genetic material, which determines particle size, and they can be obtained in high yields by simply growing and harvesting infected cells/organisms. However, working with infectious virus particles poses serious health and environmental safety risks and may require costly containment measures, depending on the virus of interest.[6, 7] With this in mind, it may be preferrable to work with virus-like particles composed of the viral coat proteins without the viral genome.

One of the most studied viral templates is tobacco mosaic virus.[8] The native virus forms helical rod-shaped particles composed of ~2130 copies of the coat protein. The particles are 300 nm in length and 18 nm in diameter with a 4 nm central channel. The viral RNA is encapsidated near the inner radius.[9] Tobacco mosaic virus coat protein (TMV-cp) is a 158 amino acid protein with a mass of approximately 17.5 kDa. In the absence of viral RNA, TMV-cp self-assembles into several different structures depending mainly on pH and ionic strength (Fig. 1). Above neutral pH and at low to moderate ionic strength, the protein exists as a mixture of monomers and small oligomers. Around pH 7.0-6.5, TMV-cp assembles into achiral, bilayer disks composed of 17 monomers per layer, 18 nm in diameter with a 4 nm central channel. At high ionic strength and non-acidic pH, these disks can stack on top of

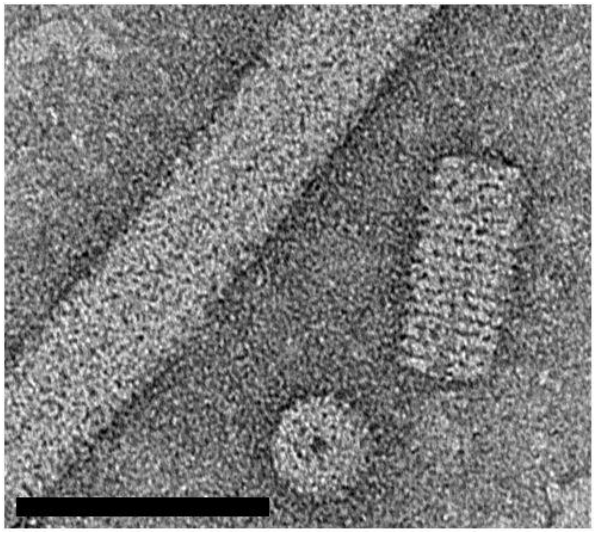

Figure 1. TEM image showing a helical rod, disk, and stacked disk aggregate. Scale bar is 50 nm.

each other to form non-helical, achiral, rod-like assemblies. In acidic pH the disks stack together and rearrange to form helical, chiral rods, retaining the same diameter and central channel.[10, 11] The stacked disks and helical rods are distinguishable in transmission electron microscopy (TEM) by the transverse striations visible in stacked disks.[12] Helical rod assembly follows a cooperative assembly model, which leads to a bimodal distribution of long rods and small particles (disks and short stacked disks), with few particles at intermediate sizes. While TMV-cp is a promising template for nanomaterials, controlling the multiple assembly states can be challenging, especially when adding additional components with different stability requirements. Apart from adjusting pH and ionic strength, mutating the coat protein has been the main method employed to control TMV-cp self-assembly, with numerous mutants designed to stabilize either the disk or rod forms.[13-16] Herein we describe a simple cosolvent-based method to modify the assembly characteristics of TMV-cp.

The use of hydrophobic cosolvents to control assembly of macromolecular components is well-established with many other systems, including lipids, synthetic polymers, and peptides, but has not previously been investigated with virus-like particles.[17-20] The present work focuses on the effect of common alcohols as cosolvents on TMV-cp. Alcohol cosolvents exert a variety of effects on solvent and protein structure. At low concentrations, single alcohol molecules remain dispersed and have a small hydration shell of structured water molecules. As alcohol content increases, the hydration shells begin to overlap, leading to an extensive hydrogen bonding network and significantly reduced mobility of water molecules. Beyond this point, alcohol molecules begin to cluster together and eventually alcohol becomes the bulk phase with small water clusters.[21, 22] These changes in solvent structure reduce the solvent permittivity and change solute pK_a and hydration number.[23, 24] Additionally, alcohol-protein interactions can replace protein-protein

interactions, altering protein structure, and even denaturing proteins.[25] In the case of TMV-cp, the presence of low concentrations of alcohol prevents formation of helical rods when reducing the pH from near neutral to acidic pH, where rods would be expected to form. At higher alcohol concentrations, stacked disks become a major component, with increased hydrophobicity leading to longer stacked disks. The perturbation appears to be based on the hydrophobicity of the cosolvent, with methanol having the weakest effect, and isopropyl alcohol having the strongest effect. This work highlights a simple method to control the self-assembly of virus-like particles without any permanent modifications to the protein structure.

Results and Discussion

TMV-cp was assembled by dialysis from pH 8.5 to lower pH in the presence of various concentrations of ethanol. Samples were characterized by TEM and dynamic light scattering (DLS). The TMV-cp samples in this work are polydisperse and non-spherical, which complicates the interpretation of DLS data. Because DLS is a light scattering technique, the signal intensity is proportional to the 6^{th} power of the radius.[26] This means that the signal from very small particles can be difficult to detect in the presence of large particles and intensity-average DLS plots appear heavily skewed towards large particles. TMV-cp samples at low pH, which are mixtures of long rods and small disks, are affected by this issue, so in some cases, the disks are not apparent in DLS. For this reason, volume- and number-average DLS results, which are less qualitative but do not favour large particles, are available in the Supplementary Information. Another complication is that DLS measures the hydrodynamic radius of particles. TMV-cp particles are non-spherical so the particle size from DLS is expected to be significantly lower than the size from TEM, especially for rods. With these issues in mind, DLS in this work should be considered an ensemble qualitative technique to detect the presence of large particles/aggregates.

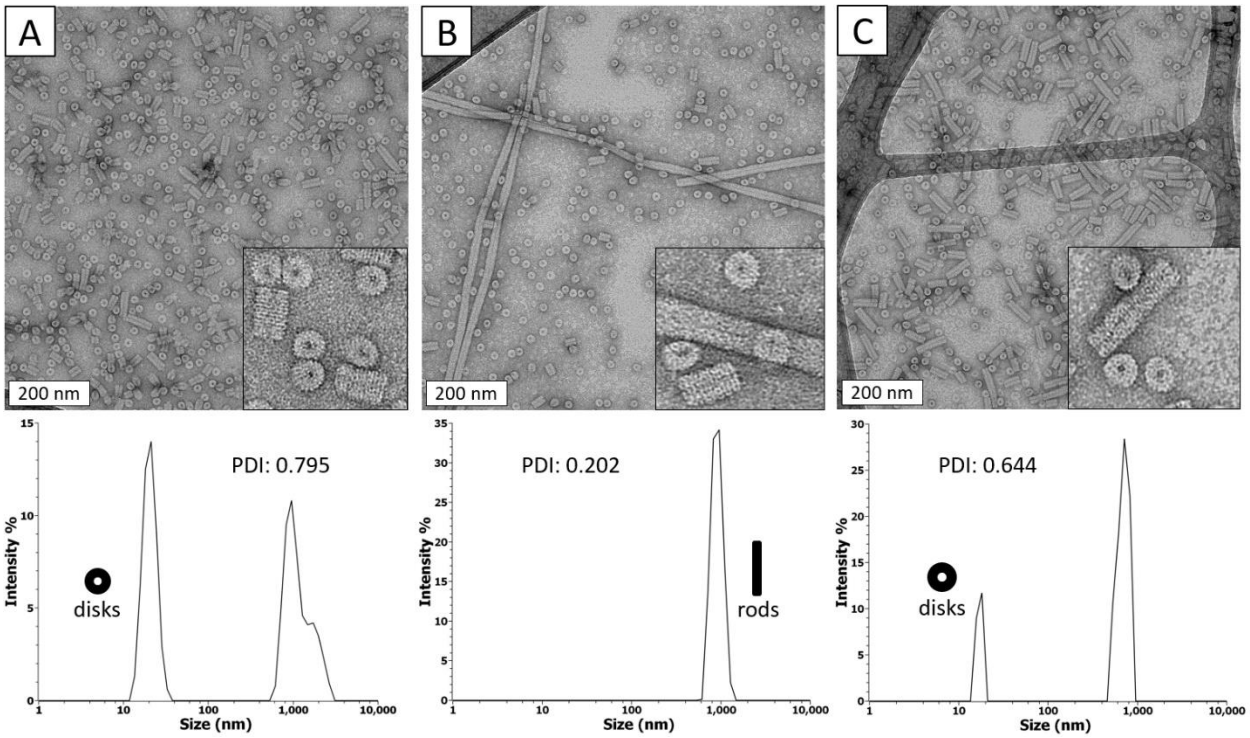

Figure 2. TEM images (top) and DLS data (bottom) for TMV-cp under different conditions. A) pH 6.8, no additive, inset shows disks and stacked disks. B) pH 5.5, no additive, inset shows helical rod, disks, and stacked disks. C) pH 5.5, 3.5 mol% ethanol, inset shows disks and stacked disks. A higher PDI (polydispersity index) indicates more polydispersity.

The effect of alcohol on TMV-cp assembly was determined by comparing alcohol-containing samples to controls at standard conditions for disk (pH 6.8) and helical rod (pH 5.5) dominated samples. All samples were characterized after 24 hours at room temperature unless otherwise noted. As expected, the pH 6.8 sample showed a mixture of disks and short stacked disks in TEM (Fig. 2). DLS showed primarily disks, with a small population of larger particles, which is likely due to dust or aggregation. In addition to disks and stacked disks, long helical rods were observed at pH 5.5 without alcohol present. At pH 5.5, ethanol concentrations below 3.5 mol% showed assembly of long, helical rods identical to those assembled with no ethanol (Fig. S1). At 3.5 mol% ethanol, helical rods were no longer observed in TEM, and DLS showed a small fraction of larger species, which indicates either minor aggregation or a small population of rods. Instead, disks became the dominant structure, with short, stacked disks forming over time. Even after 2 weeks at

room temperature, the 3.5 mol% ethanol sample at pH 5.5 was indistinguishable from a pH 6.8 sample with no ethanol (Fig. S2). As shown in Table 1, both the pH 6.8 control and pH 5.5 with 3.5 mol% ethanol samples have nearly identical frequency and average length of stacked disks. At pH 5.5, stacked disk assemblies became more common and longer with increasing ethanol concentrations (Table 1 & Fig. 3). The 5.0 and 10.0 mol% ethanol samples both showed a significant increase in the length and frequency of stacked disks. 10.0 mol% ethanol caused stacked disks to become the dominant species within 24 hours, while 5.0 mol% ethanol showed a transition in the dominant species from disk to stacked disk within 2 weeks. Helical rod assembly was recovered after removal of the ethanol by dialysis in all cases (Fig. S3). These results are consistent with a hydrophobic effect exerted by the ethanol. TMV-cp assembly has been shown to be largely driven by hydrophobic effects.[27] It is possible that the hydrophobic alcohol molecules interact favourably with the hydrophobic regions on the faces of TMV-cp disks, thereby preventing the protein-protein contacts necessary for helical rod formation and stabilizing the disk structure. Disks stack mainly through a solvent network, rather than direct protein-protein interactions, so ethanol does not disrupt the formation of stacked disks.[28, 29]

Sample	%Disks	Average Stacked Disk Length (nm)	Helical Rods
8.5, NA, Stock	89.9	23.9	No
7.5, NA	89.7	25.7	No
7.5, 3.5 EtOH	91.7	19.9	No
7.5, 5.0 EtOH	92.4	17.3	No
6.8, NA	88.6	30.3	No
6.8, NA, 2 weeks	63.4	43.8	No
6.8, 3.5 EtOH	82.0	24.1	No
6.8, 5.0 EtOH	92.2	20.8	No
5.5, NA	84.5	23.5	Yes
5.5, NA, 2 weeks	91.1	27.4	Yes
5.5, EtOH removed	90.3	37.0	Yes
5.5, 3.5 EtOH	87.3	31.1	No
5.5, 3.5 EtOH, 2 weeks	68.5	44.8	No
5.5, 5.0 EtOH	62.0	39.5	No
5.5, 5.0 EtOH, 2 weeks	24.4	55.6	No
5.5, 10.0 EtOH	26.9	73.7	No
5.5, 10.0 EtOH, 2 weeks	18.1	93.0	No
5.5, 3.5 MeOH	81.0	28.7	Yes
5.5, 5.0 MeOH	94.8	34.7	Yes
5.5, 10.0 MeOH	45.5	38.7	No
5.5, 3.5 IPA	42.3	35.7	No
5.5, 5.0 IPA	57.1	42.5	No
5.5, 10.0 IPA	65.2	60.7	No

Table 1. Particle statistics from TEM images. Samples named as "pH, additive (mol%), notes". NA is no additive. %Disks is the percent of individual disks out of all TMV-cp disks and stacked disks observed. Samples with helical rods highlighted.

The effect of pH on ethanol-perturbed assembly was also investigated. TMV-cp samples containing 3.5 and 5.0, mol% ethanol were prepared at pH 6.8 and 7.5, and 3.5, 5.0, and 10.0 mol% ethanol samples were prepared at pH 5.0 (Fig. 4A-C & Fig. S4). At pH 6.8 and 7.5, few stacked disks were observed after 24 hours. The number and length of stacked disks did increase over time in the pH 6.8 sample, but individual disks remained the dominant species. This is not surprising considering that protonation of Caspar carboxylate pairs around pH 6.5 reduces repulsion between disks, allowing larger assemblies.[30, 31] At higher pH like 6.8 and 7.5, the increased repulsion between subunits may discourage formation of stacked disks. In contrast, at pH 5.0, stacked disks were the dominant species. In 5.0 and 10.0 mol% ethanol, the pH 5.0 samples showed large raft-like clusters of stacked disks (Fig. S5). These clusters could extend for over a micron in either the axial or lateral direction. These clusters may be caused by reduced suspension stability in the presence of alcohol and reduced particle-particle repulsion near the isoelectric point (5.09) of TMV-cp.

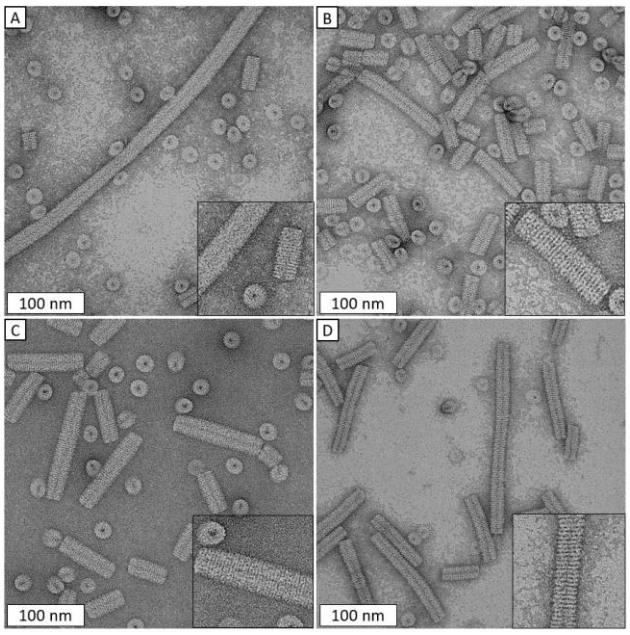

Figure 3. TEM images of A) pH 5.5, no additive, B) pH 5.5, 3.5 mol% EtOH, C) pH 5.5, 5.0 mol% EtOH, D) pH 5.5, 10.0 mol% EtOH.

To further investigate the effect of alcohols on the protein self-assembly, TMV-cp was assembled by the same procedure at pH 5.5 in the presence of methanol or isopropyl alcohol (Fig. 4D-F). As expected, a higher concentration of methanol was required to exert the same effect as ethanol on VLP assembly. 3.5 and 5.0 mol% methanol samples still showed many helical rods, but only disks and stacked disks were observed in 10.0 mol% samples. On the other hand, isopropyl

alcohol had a very strong effect on TMV-cp assembly, with 3.5 mol% completely eliminating helical rods, and higher concentrations leading to an increase in the average length of stacked disk assemblies (Fig. S6). Stacked disks at high isopropyl alcohol concentrations were longer than at high methanol concentrations, and showed large clusters in TEM.

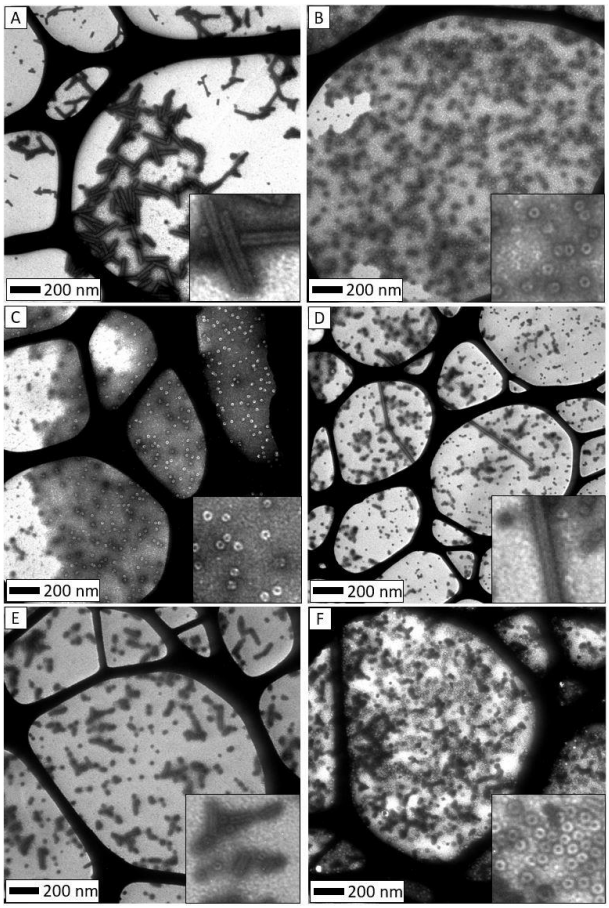

Figure 4. TEM images of TMV-cp under various conditions. A) pH 5.0, 5.0 mol% ethanol, B) pH 6.8, 5.0 mol% ethanol, C) pH 7.5, 5.0 mol% ethanol, D) pH 5.5, 5.0 mol% methanol, E) pH 5.5, 10.0 mol% methanol, F) pH 5.5, 3.5 mol% isopropyl alcohol.

Conclusions

The use of hydrophobic cosolvents to perturb assembly of TMV-cp has potential applications for nanomaterials. Low concentrations of ethanol or other alcohols can be used to stabilize the disk structure in acidic conditions, where disks would normally assemble into helical rods. This allows for the use of disks under reaction conditions that would normally favour helical rods, or with reactants that are only stable in acidic conditions. Increasing the concentration of alcohol favours achiral stacked disks at acidic pH. In this way, hydrophobic cosolvents can be used to differentiate between the chiral and achiral rod-shaped particles that TMV-cp forms. These effects appear to be caused by hydrophobic interactions between the alcohol and protein (Fig. 5). Alcohol-protein interactions may replace the protein-protein interactions required for helical rod formation. Stacked disks are formed through a solvent network, so their formation is not prevented by alcohol. Potential applications for helical

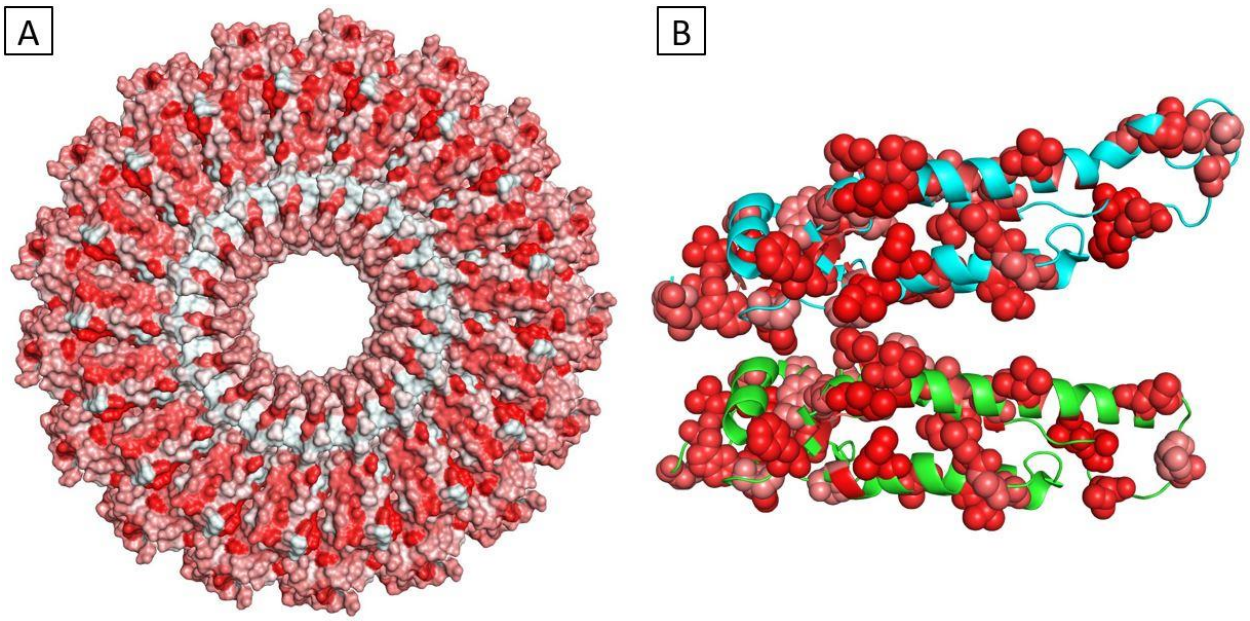

Figure 5. PyMOL[34] schematic showing A) one face of the disk, and B) side view of two layers of the disk. Hydrophobic residues are coloured in red. Based on PDB 1EI7.

and non-helical particles include templated waveguides and negative index materials.[32, 33] High alcohol content can also cause aggregation of rod-shaped particles into large raft-like structures, which could allow templating of relatively large surface areas. The effect of alcohol on TMV-cp assembly was first reported by Bruckman *et al*. They noted the formation of hexagonally-packed sheets of disks when a hexahistidine-tagged TMV-cp (6H-TMV-cp) was dialyzed to pH 5.0 in the presence of 10% ethanol.[35] At the same pH without ethanol, 6H-TMV-cp formed helical rods. However, Bruckman *et al.* only tested one concentration of ethanol and found that WT-TMV-cp assembly was unperturbed. With a more extensive investigation, the present work demonstrates that the presence of alcohols in solution has a significant effect on WT-TMV-cp assembly and suggests a mode of action that is relevant to many TMV-cp mutants. Alcohol-perturbed assembly of TMV-cp shows particular promise in combination with mutants that possess additional functionality, as demonstrated by the use of similar hexagonally-packed arrays of disks to template sheets of gold nanorings which show promise in plasmonics applications.[36] It is expected that many

TMV-cp mutants possessing interesting functionality in the disk or stacked disks phases can have that functionality extended to lower pH by simply including alcohol as a cosolvent.

Author Information

Corresponding Author

*Amy Szuchmacher Blum – McGill University, Montréal, Québec, Canada, Email: amy.blum@mcgill.ca

Author Contributions

The manuscript was written through contributions of all authors. All authors have given approval to the final version of the manuscript.

Funding Sources

This work was supported by the Canada Foundation for Innovation (CFI), Québec Centre for Advanced Materials (QCAM), and Natural Sciences and Engineering Research Council (NSERC).

Conflicts of interest

There are no conflicts to declare.

References

1. Whitesides, G. M.; Grzybowski, B. *Science* **2002**, *295* (5564), 2418-2421.
2. Busseron, E.; Ruff, Y.; Moulin, E.; Giuseppone, N. *Nanoscale* **2013**, *5* (16), 7098-7140, 10.1039/C3NR02176A.
3. Zhang, S. *Nature Biotechnology* **2003**, *21* (10), 1171-1178.
4. Lee, S.-Y.; Lim, J.-S.; Harris, M. T. *Biotechnology and Bioengineering* **2012**, *109* (1), 16-30.

5. Wen, A. M.; Steinmetz, N. F. *Chemical Society Reviews* **2016**, *45* (15), 4074-4126, 10.1039/C5CS00287G.
6. Brewer, H. C.; Hird, D. L.; Bailey, A. M.; Seal, S. E.; Foster, G. D. *Plant Biotechnol J* **2018**, *16* (4), 832-843.
7. Kimman, T. G.; Smit, E.; Klein, M. R. *Clinical Microbiology Reviews* **2008**, *21* (3), 403-425.
8. Lee, K. Z.; Basnayake Pussepitiyalage, V.; Lee, Y.-H.; Loesch-Fries, L. S.; Harris, M. T.; Hemmati, S.; Solomon, K. V. *Biotechnology Journal* **2021**, *16* (4), 2000311.
9. Harrison, B. D.; Wilson, T. M. A.; Stubbs, G. *Philosophical Transactions of the Royal Society of London. Series B: Biological Sciences* **1999**, *354* (1383), 551-557.
10. Harrison, B. D.; Wilson, T. M. A.; Klug, A. *Philosophical Transactions of the Royal Society of London. Series B: Biological Sciences* **1999**, *354* (1383), 531-535.
11. Durham, A. C. H.; Finch, J. T.; Klug, A. *Nature New Biology* **1971**, *229* (2), 37-42.
12. Ksenofontov, A.; Petoukhov, M.; Prusov, A.; Fedorova, N.; Shtykova, E. *Biochemistry (Moscow)* **2020**, *85* (3), 310-317.
13. Dedeo, M. T.; Duderstadt, K. E.; Berger, J. M.; Francis, M. B. *Nano Letters* **2010**, *10* (1), 181-186.
14. Zhou, K.; Zhou, Y.; Yang, H.; Jin, H.; Ke, Y.; Wang, Q. *Angewandte Chemie International Edition* **2020**, *59* (41), 18249-18255.
15. Brown, A. D.; Chu, S.; Kappagantu, M.; Ghodssi, R.; Culver, J. N. *Biomacromolecules* **2021**, *22* (6), 2515-2523.
16. Finbloom, J. A.; Han, K.; Aanei, I. L.; Hartman, E. C.; Finley, D. T.; Dedeo, M. T.; Fishman, M.; Downing, K. H.; Francis, M. B. *Bioconjugate Chemistry* **2016**, *27* (10), 2480-2485.
17. Lin, Y.; Penna, M.; Thomas, M. R.; Wojciechowski, J. P.; Leonardo, V.; Wang, Y.; Pashuck, E. T.; Yarovsky, I.; Stevens, M. M. *ACS Nano* **2019**, *13* (2), 1900-1909.
18. Mukherjee, S.; Deshmukh, A. A.; Mondal, S.; Gopal, B.; Bagchi, B. *J Phys Chem B* **2019**, *123* (49), 10365-10375.
19. Aliabadi, H. M.; Elhasi, S.; Mahmud, A.; Gulamhusein, R.; Mahdipoor, P.; Lavasanifar, A. *International Journal of Pharmaceutics* **2007**, *329* (1), 158-165.
20. Schnur, J. M. *Science* **1993**, *262* (5140), 1669-1676.
21. Li, R.; D'Agostino, C.; McGregor, J.; Mantle, M. D.; Zeitler, J. A.; Gladden, L. F. *The Journal of Physical Chemistry B* **2014**, *118* (34), 10156-10166.
22. Mizuno, K.; Miyashita, Y.; Shindo, Y.; Ogawa, H. *The Journal of Physical Chemistry* **1995**, *99* (10), 3225-3228.
23. Castro, G. T.; Giordano, O. S.; Blanco, S. E. *Journal of Molecular Structure: THEOCHEM* **2003**, *626* (1), 167-178.
24. Chattopadhyay, A. K.; Lahiri, S. C. *Electrochimica Acta* **1982**, *27* (2), 269-272.
25. Lousa, D.; Baptista, A. M.; Soares, C. M. *Journal of Chemical Information and Modeling* **2012**, *52* (2), 465-473.
26. Barnett, C. E. *The Journal of Physical Chemistry* **1942**, *46* (1), 69-75.
27. Butler, P. J. G. *Journal of General Virology* **1984**, *65* (2), 253-279.
28. Bhyravbhatla, B.; Watowich, S. J.; Caspar, D. L. D. *Biophysical Journal* **1998**, *74* (1), 604-615.
29. Díaz-Avalos, R.; Caspar, D. L. D. *Biophysical Journal* **1998**, *74* (1), 595-603.
30. Caspar, D. L. D.; Keiichi, N. *Advances in Biophysics* **1990**, *26*, 157-185.

31. Wang, H.; Planchart, A.; Stubbs, G. *Biophysical Journal* **1998**, *74* (1), 633-638.
32. Kuzyk, A.; Schreiber, R.; Fan, Z.; Pardatscher, G.; Roller, E.-M.; Högele, A.; Simmel, F. C.; Govorov, A. O.; Liedl, T. *Nature* **2012**, *483* (7389), 311-314.
33. Pendry, J. B. *Science* **2004**, *306* (5700), 1353-1355.
34. The PyMOL Molecular Graphics System, Version 2.4, Schrödinger, LLC.
35. Bruckman, M. A.; Soto, C. M.; McDowell, H.; Liu, J. L.; Ratna, B. R.; Korpany, K. V.; Zahr, O. K.; Blum, A. S. *ACS Nano* **2011,** *5* (3), 1606-1616.
36. Zhang, J.; Zhou, K.; Zhang, Y.; Du, M.; Wang, Q. *Advanced Materials* **2019,** *31* (23), 1901485.

ASSOCIATED CONTENT

Supporting Information

The following files are available free of charge.

Information on protein expression, purification, and characterization, as well as additional TEM images and DLS data. (PDF)